JOURNAL OF PROTEOMICS 111 (2014) 59–73

Available online at www.sciencedirect.com

ScienceDirect

www.elsevier.com/locate/jprot

Proteomic analysis identifies endoribouclease EhL-PSP and EhRRP41 exosome protein as novel interactors of EhCAF1 deadenylase☆

Itzel López-Rosas[a,b], Laurence A. Marchat[b,c], Beatriz Gallo Olvera[b,c], Nancy Guillen[d,e], Christian Weber[d,e], Olga Hernández de la Cruz[a], Erika Ruíz-García[f], Horacio Astudillo-de la Vega[g], César López-Camarillo[a,*]

[a]Autonomous University of Mexico City, Genomics Sciences Program, Mexico City, Mexico
[b]Biotechnology Program, National School of Medicine and Homeopathy, National Polytechnic Institute, Mexico City, Mexico
[c]Institutional Program of Molecular Biomedicine, National School of Medicine and Homeopathy, National Polytechnic Institute, Mexico City, Mexico
[d]Unit of Cell Biology for Parasitism, Pasteur Institute, Paris, France
[e]INSERM U786, Paris, France
[f]Translational Medicine Laboratory, National Institute of Cancerology, Mexico City, Mexico
[g]Laboratory of Translational Cancer Research and Cellular Therapy, Oncology Hospital, Medical Center Siglo XXI, Mexico City, Mexico

ARTICLE INFO

Available online 2 July 2014

Keywords:
Entamoeba histolytica
Amoebiasis
mRNA deadenylation
Deadenylase EhCAF1
Exoribonuclease EhRRP41
Endoribonuclease EhL-PSP

ABSTRACT

In higher eukaryotic cells mRNA degradation initiates by poly(A) tail shortening catalyzed by deadenylases CAF1 and CCR4. In spite of the key role of mRNA turnover in gene expression regulation, the underlying mechanisms remain poorly understood in parasites. Here, we aimed to study the function of EhCAF1 and identify associated proteins in *Entamoeba histolytica*. By biochemical assays, we evidenced that EhCAF1 has both RNA binding and deadenylase activities in vitro. EhCAF1 was located in cytoplasmic P-bodies that increased in number and size after cellular stress induced by DNA damage, heat shock, and nitric oxide. Using pull-down assays and ESI-MS/MS mass spectrometry, we identified 15 potential EhCAF1-interacting proteins, including the endoribonuclease EhL-PSP. Remarkably, EhCAF1 colocalized with EhL-PSP in cytoplasmic P-bodies in trophozoites. Bioinformatic analysis of EhL-PSP network proteins predicts a potential interaction with EhRRP41 exosome protein. Consistently, we evidenced that EhL-PSP colocalizes and physically interacts with EhRRP41. Strikingly, EhRRP41 did not coimmunoprecipitate EhCAF1, suggesting the existence of two EhL-PSP-containing complexes. In conclusion, our results showed novel interactions between mRNA degradation proteins and evidenced for the first time that EhCAF1 is a functional deadenylase that interacts with EhL-PSP endoribonuclease in P-bodies, while EhL-PSP interacts with EhRRP41 exosome protein in this early-branched eukaryote.

☆ This article is part of a Special Issue entitled: Proteomics, mass spectrometry and peptidomics, Cancun 2013. Guest Editors: César López-Camarillo, Victoria Pando-Robles and Bronwyn Jane Barkla.

* *Corresponding author at:* Genomics Sciences Program, Oncogenomics and Cancer Proteomics Laboratory, Autonomous University of Mexico City, Av. San Lorenzo 290, 03100 Mexico City, Mexico. Tel.: +52 55 5488 6661x15307.
E-mail address: genomicas@yahoo.com.mx (C. López-Camarillo).

http://dx.doi.org/10.1016/j.jprot.2014.06.019
1874-3919/

Biological significance

This study provides evidences for the functional deadenylase activity of EhCAF1 and shows a link between different mRNA degradation proteins in *E. histolytica*. By proteomic tools and pull down assays, we evidenced that EhCAF1 interacts with the putative endoribonuclease EhL-PSP, which in turn interacts with exosome EhRRP41 protein. Our data suggest for the first time the presence of two complexes, one containing the endoribonuclease EhL-PSP and the deadenylase EhCAF1 in P-bodies; and another containing the endoribonuclease EhL-PSP and the exosome EhRRP41 exoribonuclease. Overall, these results provide novel data that may help to understand mRNA decay mechanisms in this parasite.

This article is part of a Special Issue entitled: Proteomics, mass spectrometry and peptidomics, Cancun 2013. Guest Editors: César López-Camarillo, Victoria Pando-Robles and Bronwyn Jane Barkla.

1. Introduction

Polyadenylated RNA turnover is a critical determinant in eukaryotic gene expression. It results from both synthesis and degradation rates, which are continuously adjusted to cell physiological requirements. In cytoplasm, mRNA degradation is initiated by poly(A) tail shortening by deadenylases, followed by 5′-end cap removal by DCP1 and DCP2 enzymes [1]. Then, mRNA is submitted to 5′-3′ exonucleolytic digestion by XRN1. Alternatively, deadenylated mRNA can be degraded from 3′ end by exosome [2]. Alterations of any regulatory elements participating in these reactions can modify both mRNA stability and deadenylation rate, indicating that poly(A) tail shortening is a rate-limiting step in mRNA decay [3,4].

Deadenylation is performed by multiple poly(A) ribonucleases. CCR4 and POP2 proteins are the main deadenylases in *Saccharomyces cerevisiae* [5,6]. Higher eukaryotic cells have one homologue of yeast CCR4, whereas three POP2 homologues (CAF1, CAF1-like and CALIF) have been identified in human [7–9]. PAN2/PAN3 and PARN are additional poly(A) ribonucleases that participate in specific deadenylation events [10,11]. Interestingly, CAF1 and CCR4 have been involved in other cellular processes. In yeast, their association with five NOT proteins, CAF40 and CAF130 polypeptides, forms the CCR4–NOT complex, which interacts with TBP and TFIID transcription factors, establishing a functional link between mRNA synthesis and degradation [12]. CAF1 also participates in cell cycle regulation interacting with BTG1/2 and ANA/BTG3 anti-proliferative proteins [13,14]. In addition, deadenylase activity of CCR4–NOT complex contributes to DNA damage response in yeast through interactions with DUN1, MRC1, RAD9, and RAD17 checkpoint factors [15]. CAF1 also regulates mRNA poly(A) tail length of Crt1 transcription factor, which controls several DNA damage-induced genes [16]. In addition, PUF proteins that bind 3′ untranslated region (UTR) triggering mRNA decay or translational repression, physically bind POP2 deadenylase in yeast and stimulate the recruitment of CCR4 and two other enzymes involved in mRNA regulation, namely Dcp1p and Dhh1p [17,18].

After deadenylation, the exosome complex of 3′ → 5′ exoribonucleases catalyzes the complete 3′ to 5′ degradation of deadenylated transcripts in cytoplasm. The eukaryotic core exosome is a conserved nine-subunit protein complex. In yeast and human, Rrp44 and Dis3 proteins constitutively associate with the exosome and provide the sole source of processive 3′ to 5′ exoribonuclease activity [19,20]. In addition to its role in RNA decay, the exosome also participates in the processing of 3′ extended precursor molecules to mature stable RNAs, such as small nucleolar and small nuclear RNAs (snoRNAs, snRNAs) and ribosomal RNAs (rRNAs) [21,22]. Exosome activities are regulated through association with other protein complexes, such as SKI-complex factors [23], as well as TRAMP, a polymerase complex that primes structured RNA for degradation [24,25].

There is increasing data evidencing that mRNA degradation occurs in specialized cytoplasmic foci known as mRNA processing bodies (P-bodies) that are enriched in RNA substrates and mRNA turnover proteins. Although the complete protein inventory of P-bodies has not been defined, most proteins involved in the 5′-3′ mRNA-decay pathway, including decapping enzymes, 5′-3′ exonucleases and poly(A) ribonucleases, have been described as components of P-bodies, while the absence of proteins that function in the 3′-5′ decay is remarkable [26,27]. To date, the exosome and SKI-complex factors have not been detected in P-bodies [28].

As in other protozoan parasites, posttranscriptional regulation of gene expression and mRNA degradation mechanisms are poorly understood in *Entamoeba histolytica*, the protozoan parasite responsible for human amoebiasis that affects 50 million people worldwide [29]. Recently, we have reported that mRNA decay machineries, including mainly decapping and deadenylation activities are generally well conserved in *E. histolytica* [30]. We also evidenced that several proteins involved in mRNA degradation, namely the EhXRN2 exoribonuclease, the EhDCP2 decapping enzyme, the EhCAF1 deadenylase and the EhAGO2-2 protein involved in RNA interference, are enriched in cytoplasmic P-body like structures in trophozoites [30,31]. Because of the relevance of poly(A) tail removal in mRNA decay, it is of prime interest to characterize the enzymes involved in deadenylation as they are likely to be target of regulators affecting mRNA stability. Here, we report the functional characterization of a deadenylase in *E. histolytica* and provide experimental evidences for potential EhCAF1 partners, which may help to understand mRNA decay mechanisms in this early-branched protozoan parasite.

2. Material and methods

2.1. Ethics statement

This study was carried out in strict accordance with the recommendations of the Guide for the Use of Laboratory

Animals of the Investigation Center and Advanced Studies of the National Polytechnic Institute (CINVESTAV-IPN). Protocol and experiments were approved by the Institutional Animal Care of CINVESTAV-IPN. Animals were kept in environmentally controlled animal facilities. All surgeries were performed under sodium pentobarbital anesthesia, and all efforts were made to minimize suffering.

2.2. Biocomputing

The previously identified EhCAF1 protein [31] was compared to homologous proteins from other organisms by BLAST-P. CAF1 amino acid sequences from diverse organisms were aligned by ClustalW software to identified conserved residues and domains. Structural and evolutionary relationships were analyzed through PSI-BLAST [32]. Three-dimensional structure of EhCAF1 was predicted by Swiss model using yeast POP2 crystal structure (PDB1UOC) as template.

2.3. *E. histolytica* cultures

Trophozoites (strain HM1-IMSS) were axenically cultured in TYI-S-33 medium [33]. For DNA damage induction, trophozoites (3.0×10^6) were irradiated with 254 nm UV-C at 150 J m^{-2} for 8 s using a UV-Stratalinker1800 device (Stratagene) as previously described [34]. Heat shock was done by incubating trophozoites at 42 °C for 3 h as reported [35]. The generation of nitric oxide in trophozoites was performed as previously described [36,37]. Briefly, amoebas (1×10^6) were incubated in TYI-S33 medium for 1 h in the presence of 1 mM sodium nitropusside (Sigma-Aldrich). Cells in logarithmic phase of growth were used in all experiments.

2.4. Cloning of *Ehcaf1*, *EhL-PSP* and *Ehrrp41* genes

The full-length *Ehcaf1* gene (EHI_048150) was PCR amplified from *E. histolytica* (HMI:IMSS strain) genomic DNA using Ehcaf1-S (5′-CCGGATCCTTTATGAATATTAACGCCTCA-3′) and Ehcaf1-AS (5′-CCAAGCTTAAATTTCAATACAAGGCTAAT-3′) primers. The full-length (384 nt) *EhL-PSP* gene (EHI_087570) was PCR amplified using sense L-PSP-S (5′-CCCGGATCCAT GAGTAAATTAACTGTTGTT-3), and antisense L-PSP-AS (5′-CCCGGTACCTTAGAGAGTAGCAATGCA-3′) primers. The full-length (717 nt) *Ehrrp41* gene (EHI_040320) was PCR amplified using *Ehrrp41-S* (5′-CCC GGATCCATGGAATATATTTCTCCA-3′), and *Ehrrp41-AS* (5′-CCCAAGCTTTCAAAT AGTTTGATAT GA-3′) primers. *Bam*HI, *Kpn*I and *Hind*III restriction sites are underlined. *Ehcaf1* gene was cloned into the pGEX-6P1 vector (GE Life Sciences), while *EhL-PSP* and *Ehrrp41* genes were individually cloned into the pRSET-A expression vector (Invitrogen). Plasmid constructions were automatically sequenced in an ABI-PRISM 310 sequencer (Applied Biosystems).

2.5. Expression and purification of recombinant EhCAF1, EhL-PSP and EhRRP41 proteins

The recombinant EhL-PSP and EhRRP41 proteins were individually expressed in *Escherichia coli* BL21 (DE3) pLysS strain as 6x-His-tagged fusion proteins. After induction with 1 mM isopropyl-beta-D-thiogalactopyranoside (IPTG) for 3 h at 37 °C, cells were disrupted by sonication at 4 °C. Soluble proteins were purified near to homogeneity under native conditions through Ni-NTA affinity chromatography according to manufacturer recommendations (Qiagen). Identity of purified recombinant proteins was confirmed by Western blot assays using anti-6x-His-tag antibodies (1:1000, Roche) and detected by ECL-Plus system (Amersham). The recombinant EhCAF1 protein was expressed as a GST-tagged fusion protein in bacteria treated with 1 mM IPTG for 3 h and 6 h, and purified near to homogeneity through Glutathione Sepharose High Performance affinity chromatography, according to manufacturer recommendations (GE Healthcare).

2.6. Generation of antibodies and Western blot assays

Purified EhCAF1, EhRRP41 and EhL-PSP proteins were submitted to SDS-PAGE, electroeluted from Coomassie stained gels and used to immunize pathogen free New Zealand male rabbits or BALB/c mice, respectively. An initial dose of 150 μg (rabbit) or 20 μg (mouse) of recombinant proteins in complete Freund's adjuvant (Gibco) was subcutaneously inoculated into animals. Four additional doses of 100 μg (rabbit) or 20 μg (mouse) in incomplete Freund's adjuvant (Gibco) were injected each 15 days by the same via. One week after the last immunization, animals were bled, IgGs were purified through protein G sepharose chromatography and tested for reactivity against recombinant fusion proteins (30 μg/lane) in Western blot assays. Membranes were incubated with immune serum (1:1000) in 2% nonfat dry milk and 0.05% Tween-20 in PBS pH 7.4 overnight at 4 °C. Proteins were developed by peroxydase-conjugated secondary antibodies (1:6000, Jackson) and detected by the ECL-Plus system. Western blot assays using nuclear and cytoplasmic protein extracts obtained from HM1-IMSS trophozoites.

2.7. Nuclear and cytoplasmic protein extracts

Nuclear (NE) and cytoplasmic (CE) protein extracts were prepared from HM1:IMSS trophozoites according to Schreiber's protocol with some modifications [38,39]. Briefly, 4×10^6 trophozoites were harvested, washed twice with cold phosphate-buffered saline, pH 6.8, and resuspended in 400 μl cold Buffer A (10 mM Hepes, pH 7.9, 10 mM KCl, 0.1 mM EDTA, 0.1 mM EGTA, 1 mM dithiothreitol, 0.5 mM phenylmethylsulfonyl fluoride) containing protease inhibitors (Complete, Roche Molecular Biochemicals) and incubated 15 min at 4 °C. Then, trophozoites were centrifuged at 8000 ×*g* for 5 min at 4 °C, the supernatant corresponding to CE was aliquoted and stored at −70 °C until use. Nuclei were lysed by incubation and agitation in vortex for 40 min at 4 °C in 100 μl Buffer C (20 mM Hepes, pH 7.9, 0.4 M NaCl, 1 mM EDTA, 1 mM EGTA, 1 mM dithiothreitol, 1 mM phenylmethylsulfonyl fluoride) in the presence of protease inhibitors. After centrifugation at 21,000 ×*g* for 10 min at 4 °C, the supernatant corresponding to NE was aliquoted and stored at −70 °C until use. Protein concentration was determined by the Bradford method [40].

2.8. RNA electrophoretic mobility shift assays

RNA electrophoretic mobility shift assays (REMSA) were performed using a 256 nt RNA probe corresponding to the 3′

UTR of the *EhPgp5* gene [41]. RNA probe was [α-^{32}P] UTP-labeled by in vitro transcription using T7 RNA polymerase (Promega). EhCAF1 protein (5 nM) and RNA probe (5×10^5 cpm) were incubated in binding buffer for 15 min at 4 °C in the presence or absence of specific (50-fold molar excess of unlabeled homologous RNA probe) and unspecific (tRNA) competitors (150, 250 and 350-fold molar excess). RNA-protein complexes were resolved through 6% non-denaturing PAGE. Gels were vacuum-dried, and radioactive complexes were detected in a Phosphor Imager apparatus.

2.9. In vitro deadenylation assays

Poly(A_{50}) RNA probe (256 nt) corresponding to the 3′UTR of the *EhPgp5* gene [41] was obtained by in vitro transcription using T7 RNA polymerase (Promega; 15 U), 2 μg DNA template, 100 mM DTT, 20 U RNasin and 0.5 mM rNTPs. Reactions were incubated for 1 h at 37 °C. Deadenylation assays were performed in buffer A (20 mM Tris/Cl (pH 7.0), 150 mM NaCl, 2 mM $MgCl_2$, 5 U RNasin, and 5 μg RNA substrate) and EhCAF1 protein. A volume of 20 μl of the reaction mixture was incubated at 30 °C for 15, 30 and 60 min. Reactions were stopped by the addition of formamide/EDTA buffer and loaded into a 7 M urea/18% polyacrylamide (19:1) gel that was stained with toluidine blue. As controls, the degradation assay was performed without the addition of EhCAF1 or in the presence of yeast POP2 deadenylase.

2.10. Immunofluorescence and laser confocal microscopy

Trophozoites were cultured on cover slides, fixed with 4% paraformaldehyde at 37 °C for 30 min and permeabilized with 0.5% Triton-X100 in PBS 1× at 37 °C for 40 min. Then, cells were blocked in 2% BSA for 60 min at 37 °C, washed three times with PBS 1× and incubated with anti-EhCAF1, and anti-EhL-PSP antibodies generated in rabbit, or with mouse anti-EhRRP41 and the previously described EhXRN2 antibodies [31] in a dilution 1:100 at 37 °C for 1 h. Cells were washed three times and incubated with fluorescein-labeled secondary antibodies (1:200) at 37 °C for 1 h. Finally, DNA was counterstained with 4′-6-diamidino-2-phenylindole (DAPI, 5 mg/ml) for 1 min at room temperature. Samples were analyzed through an inverted microscope attached to a laser confocal scanning system Leica TCS SP2 (Leica, CO).

2.11. Pull-down assays

The purified GST-EhCAF1 protein (4 mg) was mixed with *E. histolytica* protein extracts (100 μg) that were previously incubated with other Glutathione Sepharose beads for 30 min to eliminate non-specific protein interaction, and incubated with Glutathione Sepharose beads (GE Healthcare) at 4 °C with gentle agitation for 3 h. Then, glutathione beads were collected by brief centrifugation, washed three times with washing buffer (20 mM HEPES (pH 7), 0.01% Nonidet P40, 100 mM KCl, 4 mM MgAc, 1 mM EDTA, 1 mM DTT) and resuspended in SDS-PAGE sample buffer. Finally, EhCAF1 interacting proteins were separated by SDS-PAGE and identified by tandem mass spectrometry (ESI-MS/MS).

2.12. Tandem mass spectrometry (ESI-MS/MS)

Protein bands were excised from Coomassie blue stained polyacrylamide gels, washed with 50% (v/v) methanol, 5% (v/v) acetic acid for 2 h and then, with deionized water. Gels were soaked for 10 min in 100 mM ammonium bicarbonate, cut into small pieces, dehydrated with 100% acetonitrile and vacuum-dried. In gel digestion was performed by adding 30 μl modified porcine trypsin solution (Promega, Madison, WI, USA) at 20 ng/μl in 50 mM ammonium bicarbonate followed by overnight incubation at room temperature. Peptides were extracted with 50% (v/v) acetonitrile, and 5% (v/v) formic acid twice for 30 min. Mass spectrometric analysis was carried out on a 3200 Q TRAP hybrid tandem mass spectrometer (Applied Biosystems/MDS Sciex, Concord, ON, Canada), equipped with a nanoelectrospray ion source (NanoSpray II) and a MicroIonSpray II head. The instrument was coupled on-line to a nanoAcquity Ultra Performance LC system (Waters Corporations, Milford, MA). Mass calibration of the hybrid triple quadrupole linear ion trap spectrometer was done with polypropylene glycol standard solutions. The instrument was then tuned and tested using [Glu1]-fibrinopeptide B (Sigma). Samples were desalted by injection onto a Symmetry C_{18} UPLC trapping column (5 μm, 180 μm × 20 mm, Waters Corporations) and washed with 0.1% formic acid in 100% Milli Q water. Peptides were separated on a BEH, C_{18} UPLC column (1.7 μm, 75 μm × 100 mm, Waters Corporations) equilibrated with 2% acetonitrile, 0.1% formic acid using a linear gradient of 2–70% acetonitrile, 0.1% formic acid. Spectra were acquired in automated mode using Information Dependent Acquisition (IDA), which involves switching from MS to MS/MS mode on detection of +2 to +4 charged species. The precursor ions were fragmented by collisionally-activated dissociation (CAD) in the Q2 collision cell. Collision voltages were automatically adjusted based upon the ion charge state and mass using rolling collision energy. Data interpretation and protein identification were performed with the MS/MS spectra data sets using the MASCOT search algorithm (Version 1.6b9). Trypsin was used as the specific protease and one missed cleavage was allowed with tolerances of 0.5 Da for the precursor and 0.3 Da for the fragment ion masses. Carbamidomethyl-cysteine and methionine oxidation were used as the fixed and variable modifications, respectively. A protein "hit" was accepted as a valid identification when at least two MS/MS spectra matched at the 95% level of confidence ($p < 0.05$). Ion score is $-10*\mathrm{Log}(P)$, where P is the probability that the observed match is a random event. The threshold ion score in the above conditions was 41 for $p < 0.05$.

2.13. Immunoprecipitation assays

Assays were performed as described [31,42] with minimal modifications. Cytoplasmic proteins from *E. histolytica* (100 μg) were diluted in 300 μl HNTG buffer (20 mM Hepes pH 7.5, 150 mM NaCl, 0.1% Triton, 10% glycerol), and incubated with 10 μl protein G beads (Sigma) for 30 min at 4 °C. Non-specific interacting proteins were excluded by centrifugation at 1000 ×*g* at 4 °C for 5 min. The supernatant was incubated with either anti-EhCAF1 antibodies (1:100) or anti-EhL-PSP and anti-EhRRP41 antibodies (1:100) for 3 h at 4 °C. Following

incubation, protein G-Sepharose beads were added to the samples and incubated for 16 h at 4 °C. Immunoprecipitated proteins were collected by centrifugation, washed three times with HNTG buffer, and then separated through 12% SDS-PAGE. Proteins were transferred to nitrocellulose membranes, and detected by Western blot assays using rabbit anti-EhCAF1 and anti-EhL-PSP or mouse anti-EhRRP41 antibodies.

3. Results

3.1. EhCAF1 conserves the characteristic motifs of ribonuclease D family of proteins

We have previously reported that *E. histolytica* has a reduced number of genes that codify for a minimal mRNA deadenylation machinery [31]. Notably, we identified an intron-less gene (EHI_048150) encoding for the EhCAF1 protein, as well as five NOT protein-encoding genes, suggesting the existence of a CAF1/NOT complex lacking the major CCR4 subunit. However, no homologues for deadenylases CCR4, PARN, PAN2 nor PAN3 were identified. Comparison of EhCAF1 with related proteins from other organisms showed that it presents high identity and similarity with homologous CAF1 proteins ranging from mammalians, plants and other protozoan parasites (Table 1).

Multiple alignment of homologous CAF1 proteins showed that they share conserved motifs and critical functional amino acid residues (Fig. 1A). EhCAF1 contains the ribonuclease D family signature represented by CAF1 nuclease domain (PF004857) and the conserved DEDD residues ($D_{84}E_{86}D_{206}D_{276}$) involved in 3′ to 5′ exonuclease activity in yeast POP2 and human CAF1 proteins [6]. A less conserved exonuclease domain (PF00929), which is present in some H-like ribonucleases [43], overlaps with the ribonuclease D domain in EhCAF1 amino acid sequence. PSI-BLAST analysis of EhCAF1 sequence evidenced a clear relationship between homologous proteins from human, yeast and protozoan parasites (Fig. 1B). Predicted EhCAF1 tertiary structure exhibits the characteristic folding described for the yeast POP2 crystallographic structure [43], including the nine-α helix bundle (α1 to α9) and five central β-sheets (β1 to β5). Notably, the conserved DEDD residues that are dispersed in CAF1 domain appear clustered to the central region of EhCAF1 (Fig. 1C).

3.2. EhCAF1 is a functional deadenylase

Binding of deadenylases to RNA substrates is the first step required for poly(A) tail removal. In order to define if EhCAF1 has RNA binding and deadenylase activities in vitro, the *Ehcaf1* full-length gene was cloned into the pGEX-6P1 vector and overexpressed in bacteria as a recombinant GST-tagged fusion protein. In Coomassie blue stained PAGE gels, EhCAF1 appeared as a 61 kDa band (Fig. 2A). Then, protein was purified near to homogeneity through Glutathione Sepharose affinity chromatography and used as immunogen to obtain rabbit anti-EhCAF1 serum (Fig. 2B). In Western blot assays, the specific antibodies recognized a single 37-kDa band in cytoplasmic fraction from trophozoites, which corresponds to the expected weight for endogenous EhCAF1 protein, but no signal was detected in nuclear extracts (Fig. 2C, left panel). Cross contamination between cellular fractions was discarded using antibodies raised against the nuclear transcription factor EhPC4 (Fig. 2C, right panel).

To test the RNA binding activity of EhCAF1, we performed RNA electrophoretic mobility shift assays (REMSA) using the [α-^{32}P] UTP-labeled *EhPgp5* 3′UTR as probe [32]. Results showed that EhCAF1 was able to bind the radioactive RNA probe in vitro (Fig. 2D). Control assays showed that RNA–protein complex disappeared when specific competitor was added to reaction, whereas complex remains unchanged in the presence of unspecific competitor. Moreover, no complex was formed in control reactions using BSA or GST.

To investigate the involvement of EhCAF1 in poly(A) tail degradation, we incubated an in vitro generated poly(A_{50}) tailed RNA substrate with EhCAF1. Results showed a progressive deadenylation of the poly(A_{50}) RNA in a time dependent manner. After 15 and 30 min incubation, a short RNA ladder representing the deadenylated RNA was observed. A fully deadenylated RNA product was detected after 1 h incubation (Fig. 2E). POP2 deadenylase from yeast used as control produced a similar poly(A) + RNA degradation pattern in comparison with EhCAF1, while RNA incubated without EhCAF1 remained intact (Fig. 2F). On the other hand,

Table 1 – Comparisons of EhCAF1 with related proteins from other organisms.

Protein	Organism	Accession number[a]	E-value	I (%)	S (%)
CAF1 putative	*Plasmodium falciparum*	Q8IL36	3e−60	47	66
CAF1-like (CALIFp)	*Mus musculus*	Q9D8X5	8e−58	46	63
CAF1-like (CALIFp)	*Homo sapiens*	Q9UFF9	8e−61	46	63
Putative CAF1	*Arabidopsis thaliana*	Q9SAI2	3e−59	46	66
CAF1 subunit 8	*Xenopus laevis*	Q8AVW1	3e−59	46	62
CAF1	*Dictyostelium discoideum*	Q54NG7	4e−57	45	63
CCR4 associated factor	*Leishmania major*	Q4QBI4	9e−57	43	64
CCR4 subunit 8	*Danio rerio*	Q7SXS5	5e−59	47	63
POP2, isoform A	*Drosophila melanogaster*	Q9VTS4	7e−58	44	61
CCR4 subunit 7	*Cryptococcus neoformans*	Q5K8T6	2e−57	42	62
CAF1	*Homo sapiens*	Q9UIV1	3e−60	48	64
CCR4 subunit 7	*Oryza sativa*	Q6K8X8	2e−58	42	65
CAF 1	*Caenorhabditis elegans*	Q17345	6e−58	39	52
POP2	*Saccharomyces cerevisiae*	P39008	3e−59	32	54
CCR4–NOT transcription complex subunit 7	*Giardia lamblia*	A8BP49	2e−39	39	56
CAF1	*Trichomonas vaginalis*	A2E0P4	2e−55	44	65

[a] UniProt Knowledgebase database. I, identity. S, similarity.

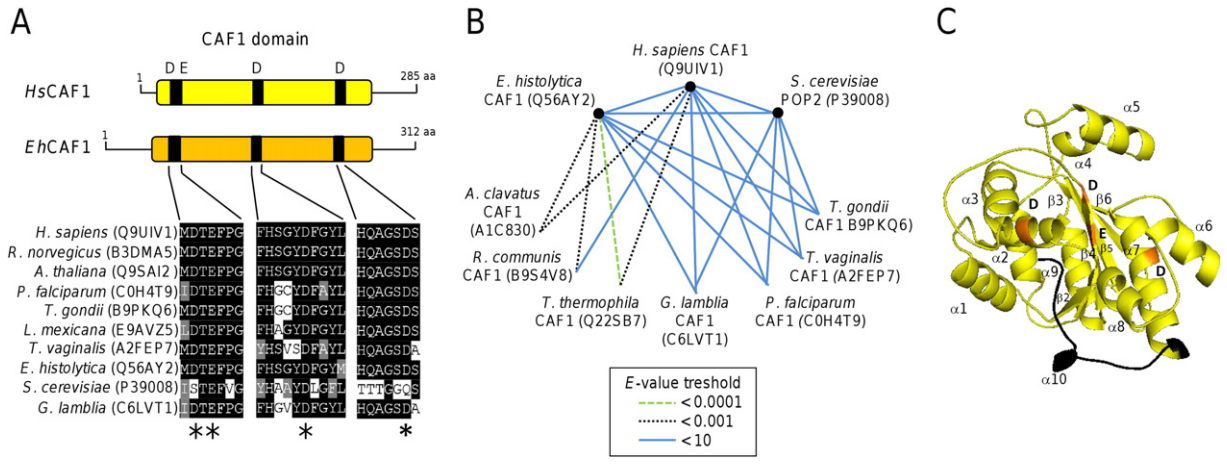

Fig. 1 – EhCAF1 has the structural motifs described in eukaryotic deadenylases. (A) Comparative molecular organization of CAF1 proteins from *Homo sapiens* and *Entamoeba histolytica*. Lower panel, ClustalW sequence alignment of conserved amino acid residues in CAF1 proteins from diverse organisms. Black boxes represent identical residues. Gray boxes denote conserved substitutions. Asterisks denote the conserved residues in DEDD motif. (B) Sequence relationships between CAF1 proteins from various organisms through PSI-BLAST analysis. The width of connected lines represents similarity level according to e-value threshold. (C) Prediction of EhCAF1 tertiary structure using the Swiss Model software and yeast POP2 deadenylase crystallographic structure (PDB1UOC) as template. Model was displayed and refined using the Pymol PBD viewer.

incubation of EhCAF1 with a poly(A)-RNA control or the use of EhPC4 protein purified from bacteria did not lead to degradation products, confirming that deadenylation activity was mediated directly by EhCAF1 rather than by trace amount of a contaminating ribonuclease from bacteria (data not shown). Taken together, these data demonstrate that EhCAF1 is a functional deadenylase in vitro.

3.3. *Cellular stress targets EhCAF1 to P-bodies*

Deadenylation is a key mechanism to modulate mRNA turnover during cellular stress [44,45]. Therefore, we investigated the distribution of EhCAF1 in permeabilized and fixed trophozoites after induction of cellular stress. As previously reported [31], results of immunofluorescence and confocal microscopy assays confirmed the cytoplasmic localization of EhCAF1, which exhibits a diffuse staining in asynchronously proliferating trophozoites. We also observed the colocalization of EhCAF1 with the exoribonuclease EhXRN2 used as a P-bodies marker [31], in some cytoplasmic *foci* in these basal culture conditions (Fig. 3, A–E). Interestingly, a differential pattern of colocalization of these mRNA degradation proteins was observed under diverse cellular stress conditions. EhCAF1/EhXRN2 containing P-bodies significantly increased in number and size after heat shock, UV-induced DNA damage and nitrosative stress in comparison to non-treated trophozoites (Fig. 3, O–T). Results showed that the average number of P-bodies increases from 1 to 5 per cell in treated trophozoites, without differences among treatments. Moreover, P-bodies' diameter increases from the 20–50 nm range in basal culture conditions to 50–300 nm range under stress conditions (data not shown). Particularly, nitrosative stress induces the formation of bigger and rounded EhCAF1/EhXRN2 containing cytoplasmic *foci* with a homogeneous distribution of both proteins in almost all P-bodies structures. Additionally we performed a Western blot assay to analyze the total amount of EhCAF1, using 100 μg of total proteins from trophozoites grown in basal conditions and submitted to cellular stress. Results showed that the expression of EhCAF1 was not significantly affected by heat shock, DNA damage and nitrosative stress (data not shown). Taken altogether, these data indicate that EhCAF1 is localized and accumulated in cytoplasmic RNA processing P-bodies after cellular stress.

3.4. *EhCAF1 interacts with the endoribonuclease EhL-PSP*

In mammalian cells, CAF1 associates with CCR4 and NOT factors to form the CCR4/CAF1/NOT complex. However, in *E. histolytica* genome, we did not find homologous genes for CCR4, PAN1, PAN2, and PARN deadenylases, which opens the possibility that EhCAF1 may interact with other proteins that surrogate the lacking deadenylases. In order to identify EhCAF1 interacting proteins, a pull-down and proteomics approach was set up. In these assays, we captured and purified proteins that interact with the GST-tagged EhCAF1 used as bait, from total protein extract used as prey. EhCAF1-interacting proteins were eluted from GST-sepharose beads and separated by SDS-PAGE (Fig. 4A). Bands were excised from gels and digested tryptic peptides were identified using ESI-MS/MS tandem mass spectrometry as described [46,47]. Proteomic analyses allowed the identification of 15 unique proteins. An overview of MS/MS peptide sequences `(ion scores), Mascot scores, and sequences coverage is shown in Table 2. Notably, the molecular weight of some identified proteins by mass spectrometry was higher than the apparent molecular weight observed in gel, indicating that polypeptides contained in excised bands were degraded during the purification process. Several proteins are involved in cell metabolism, such as glyceraldehyde-3-phosphate dehydrogenase, pyruvate

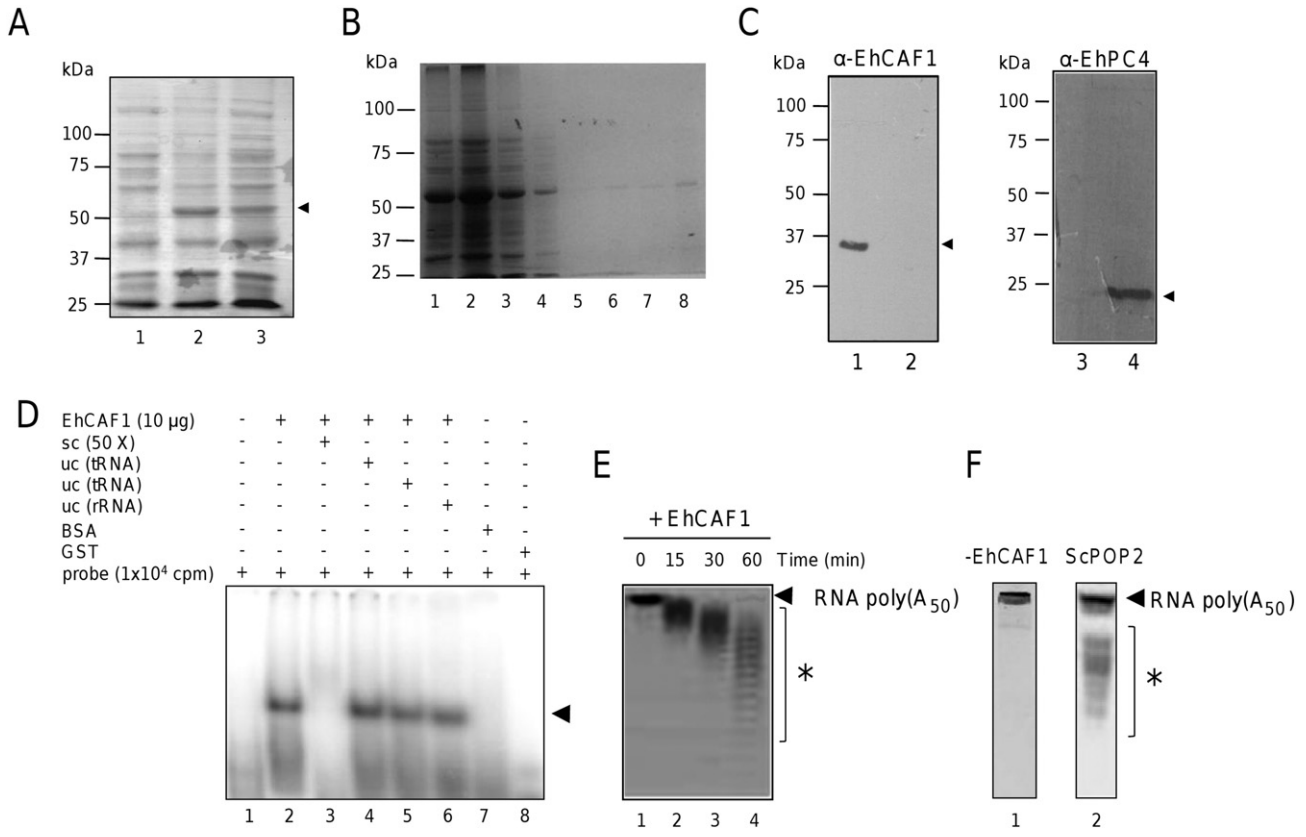

Fig. 2 – EhCAF1 is a cytoplasmic deadenylase with RNA binding and deadenylation activities. (A) Expression of recombinant 6x-His-tagged EhCAF1 protein in *E. coli* BL21(DE)pLysS. Bacterial proteins were analyzed through 10% SDS-PAGE. Lane 1, non-induced bacteria lysate; lanes 2 and 3, IPTG-induced lysate at 3 and 6 h, respectively. (B) Purification of EhCAF1 through affinity chromatography using Glutathione Sepharose beads. Fractions were analyzed through 10% SDS-PAGE. Lane 1, pellet from IPTG induced bacteria; lane 2, clarified lysate from IPTG induced bacteria; lane 3, clarified lysate flow through; lane 4–5, washes; lanes 6–8, elution fractions containing purified EhCAF1. (C) Immunodetection of EhCAF1 in cytoplasmic (lane 1) and nuclear (lane 2) fractions of trophozoites using anti-EhCAF1 antibodies. EhPC4 antibodies were used as fractioning control in cytoplasmic (lane 3) and nuclear (lane 4) fractions. Arrowheads indicate EhCAF1 (37 kDa) and EhPC4 (18 kDa) proteins. D) REMSA. The 3′UTR of *EhPgp5* RNA probe was incubated with EhCAF1 (lane 2) in the presence of specific (sc; lane 3) or unspecific competitor (uc; lane 4: 150-fold molar excess; lane 5, 250-fold molar excess and lane 6; 350-fold molar of homologous unlabeled fragment). Lane 1 free probe; Lane 7, BSA control; lane 8, GST control. Arrowhead denotes RNA-protein complex. (E) Deadenylation assay. Left panel, poly(A_{50}) RNA probe (256 nt) corresponding to the 3′UTR of *EhPgp5* gene was incubated with EhCAF1 for 1 h at 30 °C for 15 (lane 2), 30 (lane 3) and 60 (lane 4) min. Lane 1, free probe; (F) Deadenylation assay controls. Lane 1 template without EhCAF1 protein as control negative; lane 2, yeast POP2 deadenylase used as positive control. Asterisk in bracket denotes the deadenylated RNA species.

phosphate dikinase, and acetyl-CoA synthase. Others include HSP70, actin and enhancer binding protein-2. Interestingly, we also identified a putative endoribonuclease EhL-PSP (EHI_087570) (Fig. 4B), which contains the β-α-β-α-β domain (IPR013813) that is common both to bacterial chorismate mutase and members of the YjgF/Yer057p/UK114 family. Of this family of proteins, only the rat translational inhibitor protein UK114, also known as liver perchloric acid-soluble protein (L-PSP), has been demonstrated to exhibit endoribonuclease activity [48]. Because rat L-PSP represents a RNA degradation protein, we focused in the homologous L-PSP protein of *E. histolytica* for additional studies.

3.5. *EhCAF1 colocalizes with EhL-PSP in trophozoites*

We first investigated the cellular localization of EhL-PSP in trophozoites. In order to generate specific antibodies, the recombinant 6x-His-tagged EhL-PSP polypeptide was expressed with IPTG in bacteria (Fig. 4C), purified by Ni-NTA affinity chromatography and used as immunogen in mouse to obtain specific serum. Immunoblotting based on 6x-His tag and EhL-PSP antibodies showed the presence of a single 17 kDa band corresponding to the recombinant EhL-PSP fusion protein (Fig. 4C, lanes 4 and 5). Then, we studied the subcellular localization of EhL-PSP by Western blotting cytoplasmic and nuclear protein extracts from asynchronously proliferating

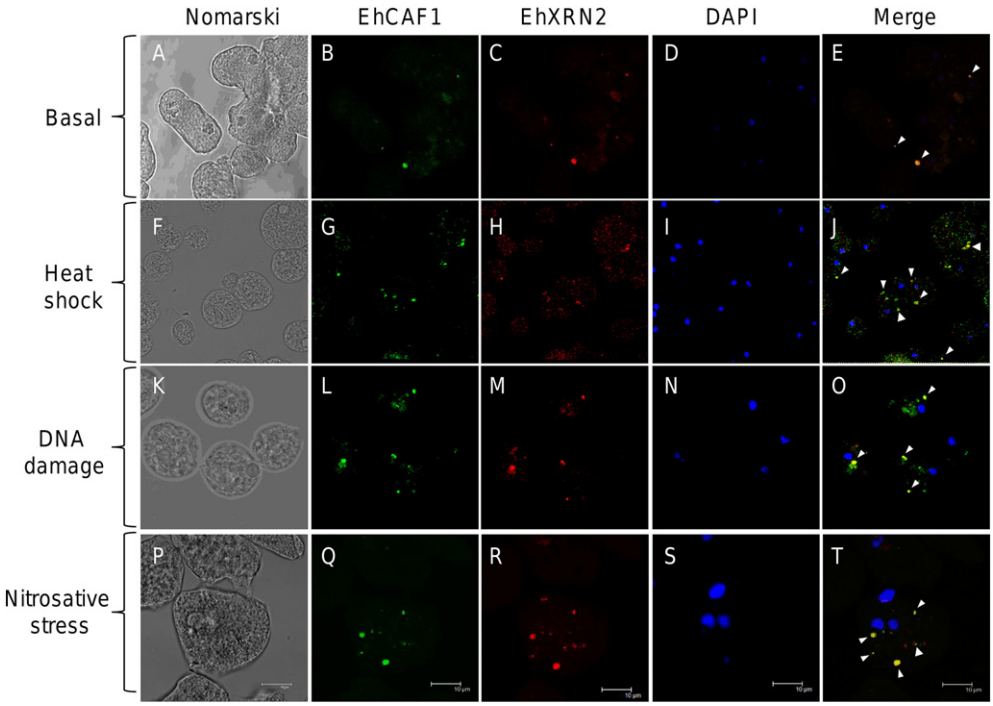

Fig. 3 – Cellular localization of EhCAF1 after induced stress in trophozoites. Fixed trophozoites were incubated with EhCAF1 and EhXRN2 antibodies, treated with FITC-labeled secondary antibodies, counterstained with DAPI and analyzed through confocal immunofluorescence microscopy. EhCAF1 immunodetection in green channel (FITC) in proliferating cells (A), after heat shock (G), DNA damage (L), and nitrosative stress (Q). EhXRN2 immunodetection in red channel in basal conditions (C), after heat shock (H), DNA damage (M), and nitrosative stress (R). (D, I, N, S), Blue DAPI channel; (E, J, O, T), Merge channels; (A, F, K, P), Nomarski images; Arrowheads indicate EhCAF1/EhXRN2-containing cytoplasmic *foci*.

trophozoites. Specific antibodies recognized a single band of ~13 kDa in cytoplasmic fraction, whereas no protein was detected in nuclear fraction (Fig. 4C). Control assays using pre-immune serum did not give any signal (data not shown). Then we sought to define the cellular localization of EhL-PSP in trophozoites using specific antibodies in immunofluorescence and confocal microscopy assays. Results indicated that EhL-PSP exhibits a homogeneous and abundant distribution in cytoplasm and plasmatic membrane of fixed permeabilized trophozoites (Fig. 4E).

To corroborate the previously observed interaction of EhL-PSP with EhCAF1, we next studied the localization of both proteins in trophozoites. Data showed that EhL-PSP and EhCAF1 display a differential pattern of cellular distribution. However, we observed that a proportion of EhL-PSP signal co-immunolocalized with EhCAF1 in common bright cytoplasmic *foci* (Fig. 4G). In contrast, we did not observe colocalization of EhCAF1 with EhL-PSP signal at the membrane (Fig. 4, G–I).

3.6. EhL-PSP colocalizes and interacts with the EhRRP41 exosome protein

In order to establish the potential functions of EhL-PSP, we first predicted its interactome using STRING algorithm [49]. Results showed the existence of an interaction network supported on predicted and experimental validated data from other organisms, in which EhL-PSP protein potentially associates with the ribonuclease EhRRP41 from exosome complex, as well as with other proteins involved in nucleotide and RNA metabolism, such as threonyl-tRNA synthetase, inosine triphosphate, guanylate kinase and fumaratehydratase (Fig. 5A). Exosome consists of a nine-subunit ring shaped structure involved in the 3′ to 5′ degradation of cytoplasmic deadenylated transcripts. Dis3 (RRP44) is the catalytic subunit responsible for both 3′ → 5′ exonucleolytic and endonucleolytic activities in yeast and human [20,50]. A recent study reported that *E. histolytica* contains seven exosome genes including Rrp41, Rrp43, Rrp46, Mtr3-Rrp42 and the catalytic subunit Dis3, as well as accessory stabilizing Rrp4, and Rrp40 proteins; but it lacks Rrp45 and Csl4 genes [30]. Because ribonucleases of exosome machinery are involved in the 3′ to 5′ decay of deadenylated transcript following CAF1-mediated deadenylation of transcripts, we decided to investigate the colocalization of EhRRP41 and EhL-PSP in trophozoites. House-made antibodies for EhRPP41 were obtained as described above for EhL-PSP. The recombinant 6x-His-tagged EhRPP41 polypeptide was expressed in bacteria (Fig. 5B), purified and used as immunogen in mouse to obtain specific serum. Western blot assays of bacteria crude extracts showed that 6x-His tag and EhRPP41 antibodies immunodetected a single 30 kDa band corresponding to recombinant 6x-His-tagged EhRPP41 fusion protein (Fig. 5C, lanes 4 and 5). In Western blot assays of cytoplasmic and nuclear extracts, EhRRP41 antibodies immunodetected the endogenous 26 kDa protein only in

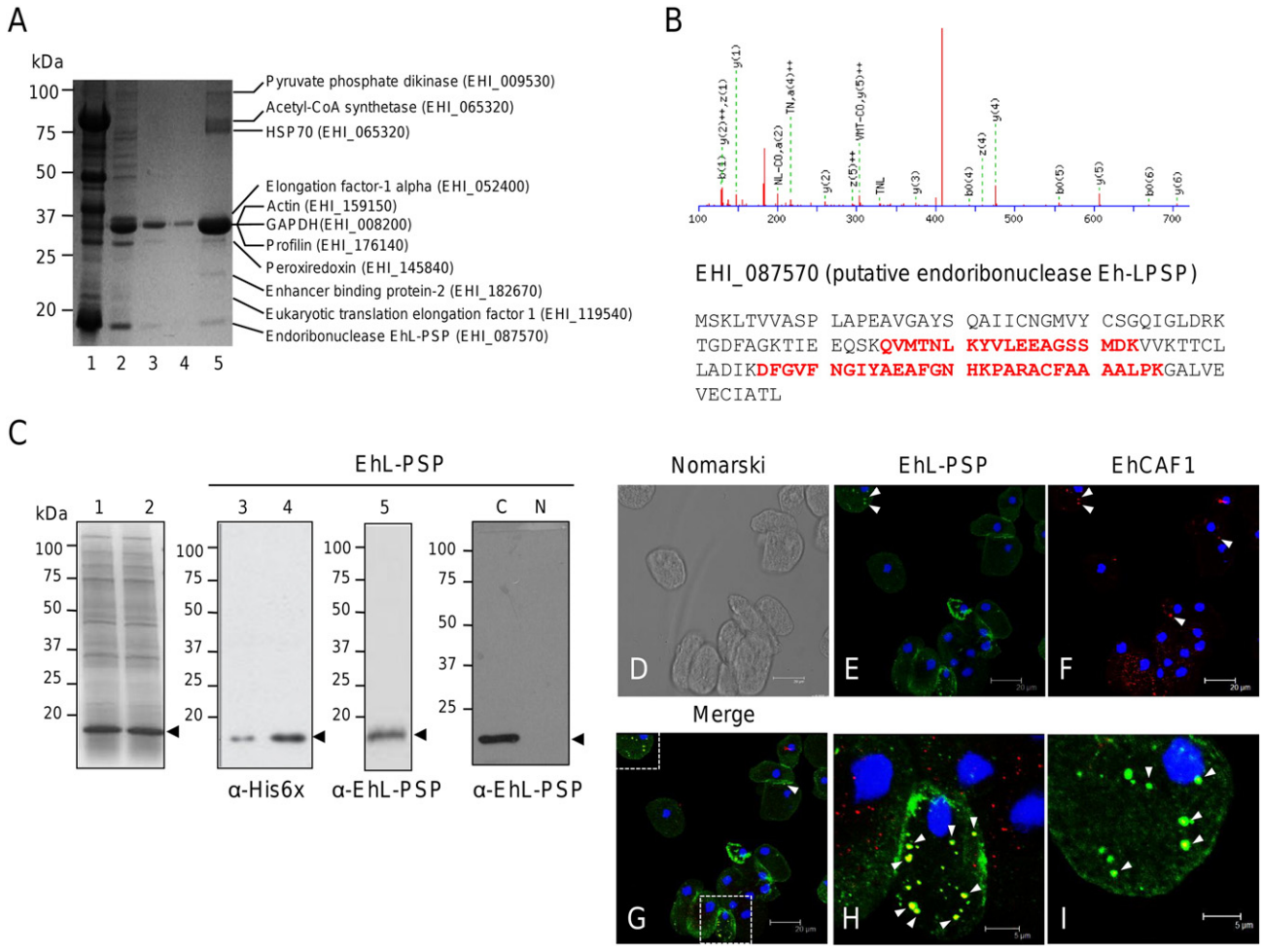

Fig. 4 – Pull-down assays and proteomic identification of EhCAF1-associated proteins. (A) Comassie stained polyacrylamide gel of GST-EhCAF1-interacting proteins identified by mass spectrometry. Lane 1, crude *E. histolytica* extract; lanes 2–4, washings; lane 5, eluted proteins. (B) MS/MS spectra for EhL-PSP. Identified sequences peptides are denoted in red. (C) Expression of recombinant 6x-His-tagged EhL-PSP protein in *E. coli* BL21(DE)pLysS. Left, Bacterial proteins were analyzed through 10% SDS-PAGE. Lane 1, non-induced bacteria lysate; lane 2, IPTG-induced lysate. Right, Immunodetection of EhL-PSP in non-induced bacteria (lane 3) and IPTG-induced bacteria (lanes 4 and 5) using anti-6x-His and anti-EhL-PSP antibodies. Immunodetection of EhL-PSP in cytoplasmic (lane C) and nuclear (lane N) fractions of trophozoites. Arrowheads indicate recombinant EhL-PSP (17 kDa) and endogenous EhL-PSP (13 kDa) proteins. (D–I) Cellular localization of EhCAF1 and EhL-PSP. Fixed trophozoites were incubated with EhL-PSP and EhCAF1 antibodies, treated with fluorescein-labeled secondary antibodies, counterstained with DAPI and analyzed through confocal immunofluorescence microscopy. (D) Nomarski image. (E) EhL-PSP immunodetection in green channel (FITC) in proliferating cells. (F) EhCAF1 immunodetection in red channel in basal trophozoites. (G, H, I) Merge channels. (H, I) Different magnifications of single cells to enhance visibility of cytoplasmic structures. Some typical *foci* are indicated with arrowheads.

cytoplasmic fraction (Fig. 5D). We next studied the cellular localization of endogenous EhRPP41 in trophozoites. Our data showed that EhRPP41 is localized in discrete cytoplasmic structures (Fig. 5E). Moreover, we detected that a small proportion (~20%) of EhL-PSP was co-immunolocalized with EhRRP41 signal in common cytoplasmic *foci* (Fig. 5H).

The physical interaction between EhL-PSP and EhRRP41 was further corroborated by immunoprecipitation assays using EhL-PSP and EhRRP41 antibodies as bait and cytoplasmic proteins from trophozoites as prey (Fig. 6A). Our, results evidenced that EhL-PSP endoribonuclease coimmunoprecipitates with EhRRP41 exoribonuclease and vice-versa. In addition, we observed that EhCAF1 coimmunoprecipitates with EhL-PSP, which is in agreement with the results of our pull down assay described above (Fig. 6A, upper panel, lanes 2 and 4). In contrast, we did not detect coimmunoprecipitation of EhCAF1 with EhRRP41, suggesting that these proteins do not have a physical interaction in trophozoites. We also found a major coimmunoprecipitation of actin protein with both baits (Fig. 6A, bottom panel, lanes 2 and 4), which is probably due to actin interaction with EhCAF1 that we previously reported [31]. As expected, no band was immunodetected when protein G coupled beads without

Table 2 – EhCAF1-interacting proteins identified by ESI-MS/MS tandem mass spectrometry.

Protein	MW/pI	Gene ID [a]	Access number [b]	Mascot score	Matched peptides	(%) coverage	Peptide sequence MS/MS (ion scores)	Function
Glyceraldehyde-3-phosphate dehydrogenase	35,991/7.04	EHI_008200	C4LVR9	1003	20	66	^{25}KDFELVAINDPFMDPK^{40} (75) ^{54}QFEGTVEAGENAIIVNGHK^{72}(79) ^{80}DPAQIGWGALGVDYVVESTGVFTTIPK^{106}(75)	Glucose metabolic process
Enolase	47,297/5.87	EHI_130700	C4LXE8	405	9	24	^{65}AVENVNTIIGPALLGK^{80}(84) ^{220}EALDLLVEAIA^{231}(86) ^{310}FTVEHGNFQIVGDDLLVTNPAR^{331}(83)	Glycolysis
Elongation factor 1-alpha	47,234/8.77	EHI_052400	C4MAC9	107	14	26	^{85}YYFTIIDAPGHR^{96}(73) ^{211}GPTLIGALDSVTPPERPVDKPLR^{233}(54) ^{253}VETGILKPGTIVQFAPSGVSSECK^{276}(32)	Protein biosynthesis
Peroxiredoxin	26,237/7.36	EHI_145840	C4M3Q0	182	17	33	^{135}LTFPLVSDIKR^{145}(62) ^{151}YGMLNVEAGIAR^{162}(92) ^{176}YIQMNDDGIGR^{186}(62)	Antioxidant and peroxiredoxin activity
Actin	41,700/5.26	EHI_159150	B1N2P0	123	13	26	^{195}GYAFTTTAER^{204}(61) ^{314}EMIQLAPPTMK^{324}(67) ^{358}EEYDESGPAIVHR^{370}(69)	Cytoesqueleton
Malic enzyme	53,286/5.92	EHI_044970	Q9NH04	1137	46	50	^{90}GNFVGVVSDSTR^{101}(72) ^{340}EAGAYIVATGR^{350}(69) ^{433}VTDLTWQQVYDIAEHDIK^{450}(75)	Malate metabolic process
Pyruvate:ferredoxin oxidoreductase	127,554/6.35	EHI_051060	C4LTX6	877	24	19	^{320}ISVLDR^{325}(56) ^{711}APAEFVQIDGK^{721}(64) ^{918}IYAAVKPLLAAEK^{930}(65)	Iron ion binding
Pyruvate phosphate dikinase	97,836/5.89	EHI_009530	Q24801	439	15	17	^{78}VFGGEENPLLVSVR^{91}(57) ^{351}TGVDMVEEGLITK^{363}(61) ^{395}GLPASPGAATGAVVFDADDAVEQAK^{419}(43)	Kinase and ligase activity
Acetyl-CoA synthetase	77,518/6.14	EHI_178960	C4LUV9	425	13	14	^{227}EFAADKPIILLK^{238}(58) ^{426}IPNFETPERIPNFETPER^{434}(57) ^{471}LIADVVADGR^{480}(65)	Energy generation
Heat shock protein 70	71,482/5.32	EHI_065320	C4M6K9	354	12	18	^{240}LVNHFIAEFKR^{250}(55) ^{349}VVQLLQDFFNGKEPNK^{364}(62) ^{365}SINPDEAVAYGAAVQAAILTGTGGK^{389}(67)	Stress response
Profilin	3228/7.63	EHI_176140	C4MB21	360	26	56	^{74}VDADEGTAMGK^{84}(62) ^{85}KGAEGISIYK^{94}(75) ^{97}QAVIIGYFSDASVSAGQNSDATYK^{120}(30)	Actin cytoskeleton organization
Endoribonuclease L-PSP	13,374/5.78	EHI_087570	C4LXT9	211	10	38	^{62}YVLEEAGSSMDK^{73}(74) ^{86}DFGVFNGIYAEAFGNHKPAR^{105}(51) ^{106}ACFAAAALPK^{115}(66)	mRNA cleavage protein synthesys inhibition
Putative fructose-1,6-bisphosphate aldolase	35,806/5.96	EHI_098570	C4LXD7	200	7	23	^{245}LESAIGIPEDQIR^{257}(56) ^{275}LAMTGSIRR^{283}(57) ^{296}QYLGPAR^{302}(48)	Glycolysis
Eukaryotic translation elongation factor 1	22,699/6.23	EHI_119540	C4M7Y2	126	4	17	^{118}IISEEQRPGTPLFNVR^{133}(54) ^{179}VGSIVAAIR^{187}(59) ^{191}GLPEGVPGLDK^{201}(22)	Protein byosinthesis
Enhancer binding protein-2	26,300/9.82	EHI_182670	C4LV48	120	4	20	^{129}EVPTEFSDNLIFVK^{142}(30) ^{143}NLAYAIKDEDLK^{154}(50) ^{180}GYGFVEVK^{187}(26)	Nucleic acid binding

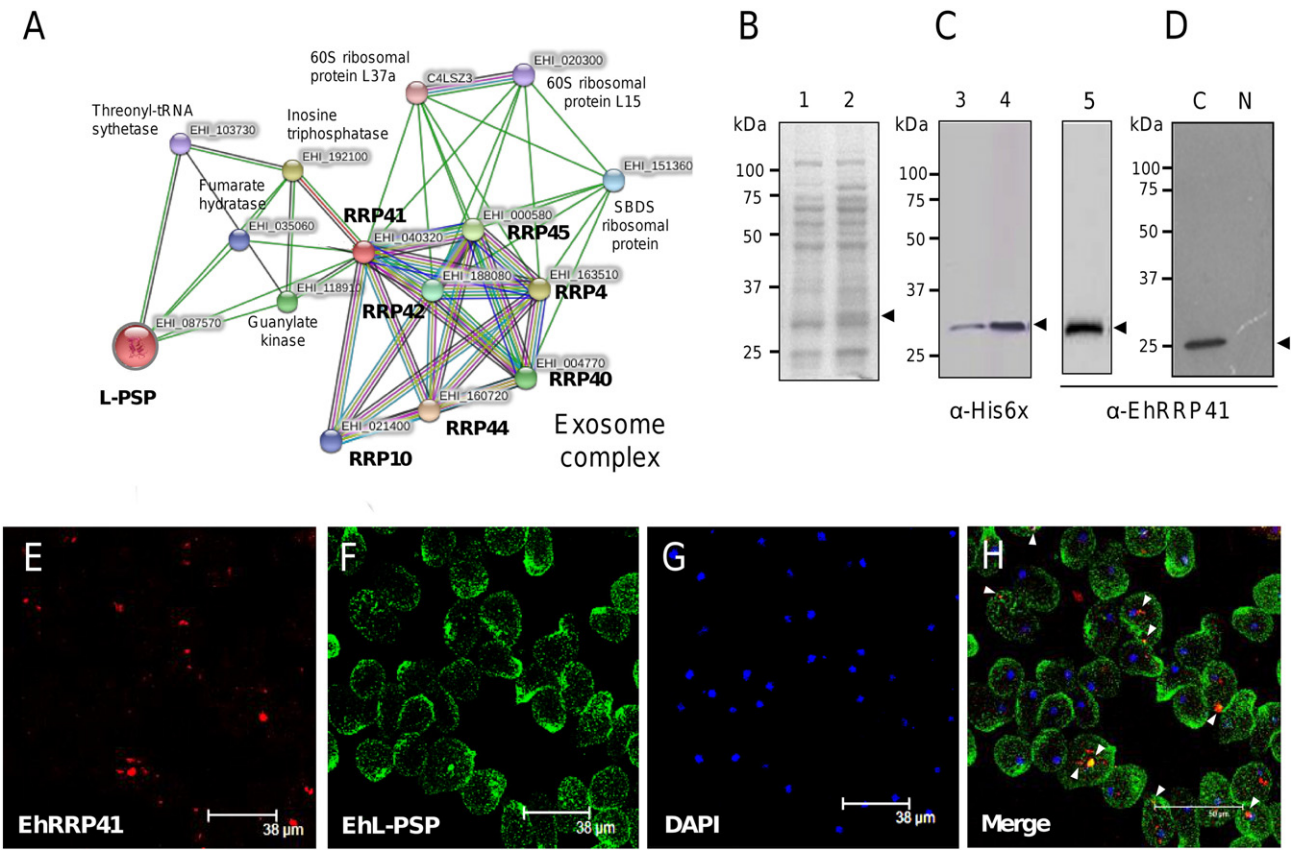

Fig. 5 – Colocalization of EhL-PSP with EhRRP41. (A) Predicted interactome for EhL-PSP protein. (B) Expression of recombinant 6x-His-tagged EhRRP41 protein in *E. coli* BL21(DE)pLysS. Bacterial proteins were analyzed through 10% SDS-PAGE. Lane 1, non-induced bacteria lysate; lane 2, IPTG-induced lysate. (C) Immunodetection of EhL-PSP in non-induced bacteria (lane 3) and IPTG-induced bacteria (lanes 4 and 5) using anti-6x-His and anti-EhRRP41 antibodies. (D) Immunodetection of EhRRP41 in cytoplasmic (lane C) and nuclear (lane N) fractions of trophozoites. Arrowheads indicate recombinant EhL-PSP (29 kDa) and endogenous EhL-PSP (26 kDa) proteins. (E–H) Cellular localization of EhRRP41 and EhL-PSP. Fixed trophozoites were incubated with EhRRP41 and EhL-PSP antibodies, treated with fluorescein-labeled secondary antibodies, counterstained with DAPI and analyzed through confocal immunofluorescence microscopy. (E) EhRRP41 immunodetection red channel (TRITC) in proliferating cells. (F) EhL-PSP immunodetection in green channel in basal conditions. (G) Nuclear staining with DAPI. (H) Merge channels. Some *foci* are indicated with arrowheads.

primary antibody and antibody anti-EhPC4 (a protein that is not related to mRNA decay mechanism) were used as negative controls. Taken altogether, these data indicate that EhL-PSP colocalizes and interacts with EhCAF1 and EhRRP41 in basal culture conditions, suggesting that EhL-PSP may have a putative role in RNA degradation in *E. histolytica*.

4. Discussion

A critical step in mRNA degradation is poly(A) tail removal. We have previously reported that *E. histolytica* has a small mRNA deadenylation machinery that is constituted by two poly(A) ribonucleases, EhCAF1 and EhCAF1-like, as well as five NOT proteins [31]. The presence of two CAF1 in *E. histolytica*, confirmed that POP2/CAF1 proteins are the most relevant deadenylases in animal cells, including protozoan parasites [51–54]. Here, we showed that EhCAF1 is a well conserved orthologue of CAF1/POP2 proteins previously described in other organisms [56]. EhCAF1 exhibits RNA binding and deadenylase activities, which suggests that it could be participating in poly(A) tail degradation in *E. histolytica*. In vitro nuclease activity has also been documented for mammalian Caf1a, Caf1b and Caf1z [57,58], *Arabidopsis* [59] and yeast [6,43] CAF1/POP2 proteins. In contrast, only few mRNA degradation proteins have been described in protozoan parasites. In *Plasmodium falciparum*, CAF1 knock-out results in accumulation of proteins involved in parasites egress and

Notes to Table 2:
[a] AmoebaDB database.
[b] Uniprot Knowledgebase.

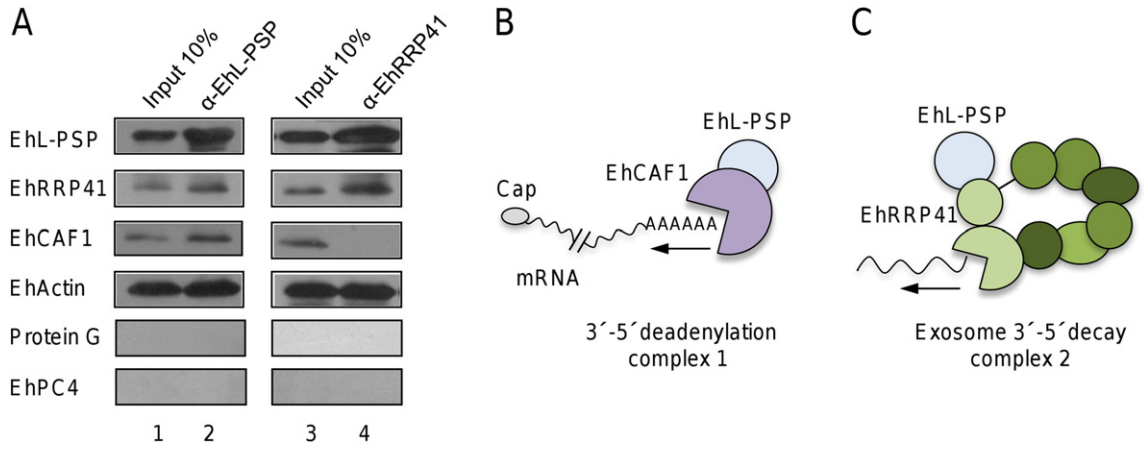

Fig. 6 – EhL-PSP and EhRRP41 interaction. (A) Inmmunoprecipitation assay. Immunoprecipitates were separated by 15% SDS-PAGE and analyzed by Western blot assay using the antibodies indicated at the left of each panel. Lanes 1 and 3, input (10% of total lysate used for immunoprecipitation); lanes 2 and 4; immunoprecipitated proteins. Protein G coupled beads without primary antibody and the EhPC4 antibody (protein unrelated to the mRNA decay mechanism) was used as negative controls. (B–C) Hypothetical working models representing the potential interactions between EhCAF1 and EhL-PSP proteins (B), and between EhL-PSP and EhRRP41 proteins (C) during mRNA decay in *E. histolytica*.

invasion of host cells [60]. *Trypanosome brucei* has a protein complex formed by CAF1, NOT1, NOT2, NOT5 and DHH1 proteins, as well as a possible homologue of Caf130. Notably, TbCAF1 is a deadenylase that is important for cell survival [55].

In *E. histolytica* trophozoites, EhCAF1 is observed diffuse in the cytoplasm as well as in small cytoplasmic dots, colocalizing with poly(A) + RNA, which is consistent with its possible role in mRNA deadenylation [1,31]. In eukaryotic cells, mRNA degradation takes place in small cytoplasmic structures called P-bodies that are also involved in mRNA storage, mRNA surveillance and RNA-based gene silencing [61]. The previous colocalization of EhXRN2, EhDCP2, EhAGO2-2 and EhCAF1 in the same cytoplasmic structures indicated that these cytoplasmic *foci* represent P-bodies-like structures in *E. histolytica* [31]. Here, we observed that the number and size of cytoplasmic *foci* containing EhCAF1 and EhXRN2 proteins vary according to cellular stress conditions, which is in agreement with several studies showing that P-bodies are dynamic structures whose number and size per cell correlate to nutrients' availability, cell cycle phase and cell proliferation [62]. Particularly, cellular stress such as heat shock, DNA damage and nitrosative stress, targets EhCAF1 and EhXRN2 to an increased number of P-body like structures in *E. histolytica*. In yeast, stress such as glucose deprivation, osmotic stress, and UV irradiation, also promotes P-bodies assembly [63]. The existence of stress granules has been described in eukaryotic cells [64,65] and more recently in this parasite [66]. Although several proteins are found in both stress granules and P-bodies, CAF1 is a specific marker of P-bodies. Therefore, the identification of EhCAF1 in the cytoplasmic *foci* described here and previously [31] confirms that they are P-body structures in *E. histolytica*.

The functional relevance of the interaction of EhCAF1 deadenylase with glyceraldehyde-3-phosphate dehydrogenase, pyruvate phosphate dikinase, acetyl-CoA synthase, HSP70, enhancer binding protein-2 and actin proteins remains to be characterized. Previously, we reported that EhCAF1 co-immunoprecipitated with EhXRN2 and colocalizes with EhXRN2 in cytoplasmic foci [31]. The fact that EhCAF1 also colocalizes with EhL-PSP, suggests that EhL-PSP co-immunolocalizes (at least in part) with EhXRN2 in common bright cytoplasmic foci. The physical interaction between EhCAF1 and the endoribonuclease EhL-PSP, as well as their colocalization in cytoplasmic *foci* confirm the role of these P-body-like structures in RNA degradation in *E. histolytica*. In our immunoprecipitation assays with EhL-PSP antibody, we detected coimmunoprecipitation of EhCAF1 and EhRRP41 proteins, suggesting that EhL-PSP interacts with both EhCAF1 and EhRRP41. However when EhRRP41 antibody was used as bait, we only detected coimmunoprecipitation of EhL-PSP, but we did not detect coimmunoprecipitation of EhCAF1 protein. This confirms that EhRRP41 physically interacts with EhL-PSP, but not with EhCAF1 in trophozoites. This result was unexpected, as EhRRP41 should bring down EhCAF1. We speculated that EhL-PSP could exist in two different complexes. Interacting with EhCAF1, EhL-PSP may be participating in the early deadenylation step of 3′-5′decay process in P-body like structures (complex 1; Fig. 6B). On other hand, interacting with EhRRP41, EhL-PSP may be part of the exosome complex involved in the last stage of 3′-5′ mRNA decay (complex 2; Fig. 6C). It is possible that the association of EhCAF1 with EhL-PSP in the first step of mRNA decay may induce conformational changes that hinder its association with EhRRP41-exosome, which may explain the absence of physical interaction between EhCAF1 and EhRRP41. After that, EhL-PSP may interact with EhRRP41-exosome to complete 3′ end RNA degradation. In human cells, exosome proteins have been described in cytoplasmic structures, together with AURE-binding proteins involved in mRNA destabilization, but not in P-bodies neither in stress granules [67]. Additional

experiments using specific antibodies should help to define if EhL-PSP and exosome EhRRP41 subunits colocalize in stress granules, P-bodies or other cytoplasmic structures.

5. Conclusions

Taken altogether, our results show that EhCAF1 is a functional deadenylase, which is targeted to P-bodies in *E. histolytica*. They also evidence novel interactions between mRNA degradation proteins in this early-branched eukaryote. Notably, we evidence for the first time that the deadenylase EhCAF1 interacts with endoribonuclease EhL-PSP in cytoplasmic P-bodies, while EhL-PSP interacts with EhRRP41 exosome protein. They also contribute to the understanding of the composition of P-body like structures that include a protein complex containing the EhCAF1 and EhL-PSP, as well as the decapping enzyme EhCDP2, the 5′ to 3′ exoribonuclease EhXRN2 and the EhAGO2-2 [31].

Conflict of interest

Author and coauthors agreed with the data presented in this manuscript, and all they contributed to the work. Authors declare no conflict of interest.

Acknowledgments

This work was supported by CONACyT, COFAA-IPN and SIP-IPN grants (Mexico). This work was also supported by Mexico–France program (SEP-CONACYT ANUIES; ECOS NORD grant M08-S02). We acknowledge the Autonomous University of Mexico City for support.

REFERENCES

[1] Chen CYA, Shyu AB. Mechanisms of deadenylation-dependent decay. WIREs RNA 2011;2:167–83.
[2] Allmang C, Petfalski E, Podtelejnikov A, Mann M, Tollervey D, Mitchell P. The yeast exosome and human PM-Scl are related complexes of 3′->5′ exonucleases. Genes Dev 1999;13:2148–58.
[3] Caponigro G, Parker R. mRNA turnover in yeast promoted by the MATalpha1 instability element. Nucleic Acids Res 1996;24:4304–12.
[4] Caponigro G, Parker R. Mechanisms and control of mRNA turnover in *Saccharomyces cerevisiae*. Microbiol Rev 1996;60:233–49.
[5] Chen J, Rappsilber J, Chiang YC, Russell P, Mann M. CL Denis. Purification and characterization of the 1.0 MDa CCR4–NOT complex identifies two novel components of the complex. J Mol Biol 2001;314:683–94.
[6] Daugeron MC, Mauxion F, Seraphin B. The yeast POP2 gene encodes a nuclease involved in mRNA deadenylation. Nucleic Acids Res 2001;29:2448–55.
[7] Albert TK, Lemaire M, van Berkum NL, Gentz R, Collart MA, Timmers HT. Isolation and characterization of human orthologs of yeast CCR4–NOT complex subunits. Nucleic Acids Res 2000;28:809–17.
[8] Tucker M, Valencia-Sanchez MA, Staples RR, Chen J, Denis CL, Parker R. The transcription factor associated Ccr4 and Caf1 proteins are components of the major cytoplasmic mRNA deadenylase in *Saccharomyces cerevisiae*. Cell 2001;104:377–86.
[9] Tucker M, Staples RR, Valencia-Sanchez MA, Muhlrad D, Parker R. Ccr4p is the catalytic subunit of a Ccr4p/Pop2p/Notp mRNA deadenylase complex in *Saccharomyces cerevisiae*. EMBO J 2002;21:1427–36.
[10] Brown CE, Sachs AB. Poly(A) tail length control in *Saccharomyces cerevisiae* occurs by message-specific deadenylation. Mol Cell Biol 1998;18:6548–59.
[11] Martinez J, Ren YG, Nilsson P, Ehrenberg M, Virtanen A. The mRNA cap structure stimulates rate of poly(A) removal and amplifies processivity of degradation. J Biol Chem 2001;276:27923–9.
[12] Badarinarayana V, Chiang YC, Denis CL. Functional interaction of CCR4–NOT proteins with TATAA-binding protein (TBP) and its associated factors in yeast. Genetics 2000;155:1045–54.
[13] Rouault JP, Prevot D, Berthet C, Birot AM, Billaud M, Magaud JP, et al. Interaction of BTG1 and p53-regulated BTG2 gene products with mCaf1, the murine homolog of a component of the yeast CCR4 transcriptional regulatory complex. J Biol Chem 1998;273:22563–9.
[14] Prevot D, Morel AP, Voeltzel T, Rostan MC, Rimokh R, Magaud JP, et al. Relationships of the antiproliferative proteins BTG1 and BTG2 with CAF1, the human homolog of a component of the yeast CCR4 transcriptional complex: involvement in estrogen receptor alpha signaling pathway. J Biol Chem 2001;276:9640–8.
[15] Traven A, Hammet A, Tenis N, Denis CL, Heierhorst J. CCR4–NOT complex mRNA deadenylase activity contributes to DNA damage responses in *Saccharomyces cerevisiae*. Genetics 2005;169:65–75.
[16] Woolstencroft RN, Beilharz TH, Cook MA, Preiss T, Durocher D, Tyers M. Ccr4 contributes to tolerance of replication stress through control of CRT1 mRNA poly(A) tail length. J Cell Sci 2006;119:5178–92.
[17] Goldstrohm AC, Seay DJ, Hook BA, Wickens M. PUF protein-mediated deadenylation is catalyzed by Ccr4p. J Biol Chem 2007;282:109–14.
[18] Goldstrohm AC, Hook BA, Seay DJ, Wickens M. PUF proteins bind Pop2p to regulate messenger RNAs. Nat Struct Mol Biol 2006;13:533–9.
[19] Liu Q, Greimann JC, Lima CD. Reconstitution, activities, and structure of the eukaryotic RNA exosome. Cell 2006;127:1223–37.
[20] Wang HW, Wang J, Ding F, Callahan K, Bratkowski MA, Butler JS, et al. Architecture of the yeast Rrp44 exosome complex suggests routes of RNA recruitment for 3′ end processing. Proc Natl Acad Sci U S A 2007;104:16844–9.
[21] Allmang C, Kufel J, Chanfreau G, Mitchell P, Petfalski E, Tollervey D. Functions of the exosome in rRNA, snoRNA and snRNA synthesis. EMBO J 1999;18:5399–410.
[22] van Hoof A, Lennertz P, Parker R. Yeast exosome mutants accumulate 3′-extended polyadenylated forms of U4 small nuclear RNA and small nucleolar RNAs. Mol Cell Biol 2000;20:441–52.
[23] Araki Y, Takahashi S, Kobayashi T, Kajiho H, Hoshino S, Katada T. Ski7p G protein interacts with the exosome and the Ski complex for 3′- to -5′ mRNA decay in yeast. EMBO J 2001;20:4684–93.
[24] Wyers F, Rougemaille M, Badis G, Rousselle JC, Dufour ME, Boulay J, et al. Cryptic pol II transcripts are degraded by a nuclear quality control pathway involving a new poly(A) polymerase. Cell 2005;121:725–37.
[25] LaCava J, Houseley J, Saveanu C, Petfalski E, Thompson E, Jacquier A, et al. RNA degradation by the exosome is

promoted by a nuclear polyadenylation complex. Cell 2005;121:713–24.
[26] Eulalio A, Behm-Ansmant I, Izaurralde E. P bodies: at the crossroads of post-transcriptional pathways. Nat Rev Mol Cell Biol 2007;8:9–22.
[27] Kulkarni M, Ozgur S, Stoecklin G. On track with P-bodies. Biochem Soc Trans 2010;38:242–51.
[28] Sheth U, Parker R. Decapping and decay of messenger RNA occur in cytoplasmic processing bodies. Science 2003;2:805–8.
[29] Stanley Jr SL. Amoebiasis. Lancet 2003;361:1025–34.
[30] López-Camarillo C, López-Rosas I, Ospina-Villa JD, Marchat LA. Deciphering molecular mechanisms of mRNA metabolism in the deep-branching eukaryote *Entamoeba histolytica*. WIREs RNA 2013. http://dx.doi.org/10.1002/wrna.1205.
[31] Lopez-Rosas I, Orozco E, Marchat LA, García-Rivera G, Guillen N, Weber C, et al. mRNA decay proteins are targeted to poly(A) + RNA and dsRNA-containing cytoplasmic foci that resemble P-bodies in *Entamoeba histolytica*. PLoS One 2012;7:e45966.
[32] Altschul SF, Madden TL, Schaffer AA, Zhang J, Zhang Z, Miller W, et al. Gapped BLAST and PSI-BLAST: a new generation of protein database search programs. Nucleic Acids Res 1997;25:3389–402.
[33] Diamond LS, Harlow DR, Cunnick CC. A new medium for the axenic cultivation of *Entamoeba histolytica* and other Entamoeba. Trans R Soc Trop Med Hyg 1978;72:431–2.
[34] López-Casamichana M, Orozco E, Marchat LA, López-Camarillo C. Transcriptional profile of the homologous recombination machinery and characterization of the EhRAD51 recombinase in response to DNA damage in *Entamoeba histolytica*. BMC Mol Biol 2008;9:35.
[35] Weber C, Guigon G, Bouchier C, Frangeul L, Moreira S, Sismeiro O, et al. Stress by heat shock induces massive down regulation of genes and allows differential allelic expression of the Gal/GalNAc lectin in *Entamoeba histolytica*. Eukaryot Cell 2006;5:871–5.
[36] Ramos E, Olivos-Garcia A, Nequiz M, Saavedra E, Tello E, Saralegui A, et al. *Entamoeba histolytica*: apoptosis induced in vitro by nitric oxide species. Exp Parasitol 2007;116:257–65.
[37] Santi-Rocca J, Smith S, Weber C, Pineda E, Hon CC, Saavedra E E, Olivos-García A, Rousseau S, Dillies MA, Coppée JY, Guillén N. Endoplasmic reticulum stress-sensing mechanism is activated in Entamoeba histolytica upon treatment with nitric oxide. PLoS One 2012;7(2):e31777.
[38] Schreiber E, Matthias P, Muller MM, Schaffner W. Rapid detection of octamer binding proteins with 'mini-extracts', prepared from a small number of cells. Nucleic Acids Res 1989;17:6419.
[39] Marchat LA, Gómez C, Pérez DG, Paz F, Mendoza L, Orozco E. Two CCAAT/enhancer binding protein sites are cis-activator elements of the *Entamoeba histolytica* EhPgp1 (MDR-like) gene expression. Cell Microbiol 2002;4:725–37.
[40] Bradford MM. A rapid and sensitive method for the quantitation of microgram quantities of protein utilizing the principle of protein-dye binding. Anal Biochem 1976;7(72):248–54.
[41] López-Camarillo C, Luna-Arias JP, Marchat LA, Orozco E. EhPgp5 mRNA stability is a regulatory event in the *Entamoeba histolytica* multidrug resistance phenotype. J Biol Chem 2003;278:11273–80.
[42] Tovy A, Siman Tov R, Gaentzsch R, Helm M, Ankri S. A new nuclear function of the *Entamoeba histolytica* glycolytic enzyme enolase: the metabolic regulation of cytosine-5 methyltransferase 2 (Dnmt2) activity. PLoS Pathog 2010;6(2):e1000775.
[43] Thore S, Mauxion F, Seraphin B, Suck D. X-ray structure and activity of the yeast Pop2 protein: a nuclease subunit of the mRNA deadenylase complex. EMBO Rep 2003;4:1150–5.
[44] Munchel SE, Shultzaberger RK, Takizawa N, Weis K. Dynamic profiling of mRNA turnover reveals gene-specific and system-wide regulation of mRNA decay. Mol Biol Cell 2011;22:2787–95.
[45] Fan J, Yang X, Wang W, Wood III WH, Becker KG, Gorospe M. Global analysis of stress-regulated mRNA turnover by using cDNA arrays. Proc Natl Acad Sci U S A 2002;99:10611–6.
[46] Fonseca-Sánchez MA, Rodríguez Cuevas S, Mendoza-Hernández G, Bautista-Pina V, Arechaga Ocampo E, Hidalgo Miranda A, et al. Breast cancer proteomics reveals a positive correlation between glyoxalase 1 expression and high tumor grade. Int J Oncol 2012;41:670–80.
[47] Díaz-Chávez J, Fonseca-Sánchez MA, Arechaga-Ocampo E, Flores-Pérez A, Palacios-Rodríguez Y, Domínguez-Gómez G, et al. Proteomic profiling reveals that resveratrol inhibits HSP27 expression and sensitizes breast cancer cells to doxorubicin therapy. PLoS One 2013;8(5):e64378.
[48] Morishita R, Kawagoshi A, Sawasaki T, Madin K, Ogasawara T, Oka T, et al. Ribonuclease activity of rat liver perchloric acid-soluble protein, a potent inhibitor of protein synthesis. J Biol Chem 1999;274:20688–92.
[49] Franceschini A, Szklarczyk D, Frankild S, Kuhn M, Simonovic M, Roth A, et al. STRING v9.1: protein–protein interaction networks, with increased coverage and integration. Nucleic Acids Res 2013;41:D808–15.
[50] Schneider C, Leung E, Brown J, Tollervey D. The N-terminal PIN domain of the exosome subunit Rrp44 harbors endonuclease activity and tethers Rrp44 to the yeast core exosome. Nucleic Acids Res 2009;37:1127–40.
[51] Temme C, Zaessinger S, Meyer S, Simonelig M, Wahle E. A complex containing the CCR4 and CAF1 proteins is involved in mRNA deadenylation in Drosophila. EMBO J 2004;23:2862–71.
[52] Schwede A, Manful T, Jha BA, Helbig C, Bercovich N, Stewart M, et al. The role of deadenylation in the degradation of unstable mRNAs in trypanosomes. Nucleic Acids Res 2009;37:5511–28.
[53] Zheng D, Ezzeddine N, Chen CY, Zhu W, He X, Shyu AB. Deadenylation is prerequisite for P-body formation and mRNA decay in mammalian cells. J Cell Biol 2008;182:89–101.
[54] Molin L, Puisieux A. *C. elegans* homologue of the Caf1 gene, which encodes a subunit of the CCR4–NOT complex, is essential for embryonic and larval development and for meiotic progression. Gene 2005;358:73–81.
[55] Schwede A, Ellis L, Luther J, Carrington M, Stoecklin G, Clayton C. A role for Caf1 in mRNA deadenylation and decay in trypanosomes and human cells. Nucleic Acids Res 2008;36:3374–88.
[56] Wahle E, Winkler GS. RNA decay machines: deadenylation by the CCR4–NOT and Pan2–Pan3 complexes. Biochim Biophys Acta 1829;2013:561–70.
[57] Wagner E, Clement SL, Lykke-Andersen J. An unconventional human Ccr4–Caf1 deadenylase complex in nuclear cajal bodies. Mol Cell Biol 2007;27:1686–95.
[58] Bianchin C, Mauxion F, Sentis S, Seraphin B, Corbo L. Conservation of the deadenylase activity of proteins of the Caf1 family in human. RNA 2005;11:487–94.
[59] Liang W, Li C, Liu F, Jiang H, Li S, Sun J, et al. The Arabidopsis homologs of CCR4-associated factor 1 show mRNA deadenylation activity and play a role in plant defence responses. Cell Res 2009;19:307–16.
[60] Balu B, Maher SP, Pance A, Chauhan C, Naumov AV, Andrews RM, et al. CCR4-associated factor 1 coordinates the expression of Plasmodium falciparum egress and invasion proteins. Eukaryot Cell 2011;10:1257–63.
[61] Cougot N, Babajko S, Seraphin B. Cytoplasmic foci are sites of mRNA decay in human cells. J Cell Biol 2004;165:31–40.
[62] Yang Z, Jakymiw A, Wood MR, Eystathioy T, Rubin RL, Fritzler MJ, et al. GW182 is critical for the stability of GW bodies

expressed during the cell cycle and cell proliferation. J Cell Sci 2004;117:5567–78.
[63] Sheth U, Parker R. Decapping and decay of messenger RNA occur in cytoplasmic processing bodies. Science 2003;300:805–8.
[64] Kimball SR, Horetsky RL, Ron D, Jefferson LS, Harding HP. Mammalian stress granules represent sites of accumulation of stalled translation initiation complexes. Am J Physiol Cell Physiol 2003;284:C273–84.
[65] Kedersha N, Anderson P. Stress granules: sites of mRNA triage that regulate mRNA stability and translatability. Biochem Soc Trans 2002;30:963–9.
[66] Katz S, Trebicz-Geffen M, Ankri S. Stress granule formation in *Entamoeba histolytica*: cross-talk between EhMLBP, EhRLE3 reverse transcriptase and polyubiquitinated proteins. Cell Microbiol 2014. http://dx.doi.org/10.1111/cmi.12273.
[67] Lin WJ, Duffy A, Chen CY. Localization of AU-rich element-containing mRNA in cytoplasmic granules containing exosome subunits. J Biol Chem 2007;282(27):19958–68.